JOURNAL OF SOLID STATE CHEMISTRY **121,** 181–189 (1996)
ARTICLE NO. 0026

Synthesis, Structure, and Characterization of Uranium(IV) Phenyl Phosphonate, $U(O_3PC_6H_5)_2$, and Uranium(IV) Pyro Phosphate, UP_2O_7

Aurelio Cabeza, Miguel A. G. Aranda, Fernando M. Cantero, Diego Lozano, María Martínez-Lara, and Sebastián Bruque[1]

Departamento de Química Inorgánica, Facultad de Ciencias, Universidad de Málaga, 29071—Málaga, Spain

Received June 12, 1995; in revised form September 11, 1995; accepted September 13, 1995

Two tetravalent uranium compounds have been characterized. The structure of a new uranium(IV) phosphonate, $U(O_3PC_6H_5)_2$, has been solved from laboratory X-ray powder diffraction data by using *ab initio* methodology. $U(O_3PC_6H_5)_2$ crystallizes in the space group $C2/m$ with $a = 9.4559(7)$ Å, $b = 5.6769(5)$ Å, $c = 14.9687(12)$ Å, $\beta = 96.539(5)$ Å, $V = 798.3(1)$ Å^3, $Z = 2$. The reliability factors were $R_{WP} = 8.0\%$, $R_P = 6.04\%$, and $R_F = 3.0\%$. The structure is lamellar, and the framework of the $U(O_3P)_2$ layers is similar to that of the α-$Zr(HPO_4)_2 \cdot H_2O$-type structure, although the symmetry of the phosphonate group is higher than that of the phosphate groups in α-$Zr(HPO_4)_2 \cdot H_2O$ and the phosphonate group in $Zr(O_3PC_6H_5)_2$. The phenyl groups are located in the interlamellar space, being inclined 10° to the *c*-axis. The phenyl rings are tilted out 53° from the *ac* plane, and they are disordered. We have also characterized this compound by UV-VIS-IR spectroscopies and thermal analysis. The thermal decomposition product is uranium(IV) pyro phosphate. This compound was identified through its X-ray powder diffraction pattern. UP_2O_7 crystallizes in the $Pa\bar{3}$ space group ($a = 8.6311(2)$ Å, $V = 642.99(4)$ Å^3, $Z = 4$). The structure belongs to the cubic ZrP_2O_7-type structure. The reliability factors were $R_{WP} = 11.7\%$, $R_P = 8.6\%$, and $R_F = 10.4\%$. Disorder has been found in the oxygen that bridges the pyrophosphate groups, leading to an angular P–O–P arrangement. The VIS-near-IR adsorption spectra revealed the uranium(IV) presence and the oxygen environment.

INTRODUCTION

The first metal organo-phosphonates described in the bibliography were tetravalent metal phosphonates. The first examples being organic zirconium phosphonates, $Zr(O_3PR)_2$ and $Zr(O_3POR)_2$ (1). In these compounds, the organic groups are joined to the zirconium phosphonate layer by covalent P–C or P–O–C bonds. Later, divalent (2), trivalent (3), and pentavalent (4) metal phosphonates were also described.

The structures and properties of these compounds are determined by the choice of metal and phosphonic acid and the reaction conditions. Metal phosphonates are very useful for ordering molecules in lamellar structures (5). These compounds are hybrid materials (organic–inorganic) and they can be prepared as polycrystalline solids, thin films, or membranes, depending upon the applications. Nowadays, there is a great deal of work in metal phosphonates due to their interesting physical and chemical properties. These compounds can act as host materials in intercalation reactions (6) and if properly functionalized they may serve as catalyst (7), ionic and electronic conductors (8), and ion exchangers (9).

To understand these properties and to rationalize the mechanism of some of these reactions it is vital to know the crystal structures precisely. Unfortunately, most of these compounds do not grow as single crystals, hence, it is necessary to use powder diffraction methodology. Although the frameworks of these materials are usually lamellar, most of them have new structures. In recent years it has been shown that crystal structures can also be determined *ab initio* (without any prior structural knowledge) by powder diffraction (10).

Sometimes, the structures of new phosphonates are related to known inorganic phosphates. For example, Clearfield and co-workers (11) have recently determined the crystal structure of $Zr(O_3PC_6H_5)_2$ by using powder diffraction data. The structure is quite similar to that of zirconium hydrogen phosphate α-$Zr(HPO_4)_2 \cdot H_2O$ (12). Another example is the structure of vanadyl phenyl phosphonate, $VO(O_3PC_6H_5) \cdot H_2O$ (13), which is related that of β-$VOPO_4$ (14).

We are currently carrying out a detailed study of some metal phosphonates. As a result, we have prepared two uranyl phosphonates (15). In this paper, we present the synthesis, crystal structure, spectroscopic characterization,

[1] To whom correspondence should be addressed.

0022-4596/96 $12.00

and thermal stability of a new tetravalent metal phenyl phosphonate, $U(O_3PC_6H_5)_2$. We will compare the structure and properties of this material with those of the Zr-analog. We have also studied UP_2O_7, as this is the thermal decomposition product of uranium(IV) phenylphosphonate. The structure of UP_2O_7 was partially studied (16) and it is known that it crystallizes in the cubic ZrP_2O_7-type structure (17). However, the position of one oxygen was not located, and we have refined the crystal structure of this compound to have a better understanding of the crystal chemistry of U(IV) phosphates and phosphonates.

EXPERIMENTAL SECTION

Uranium(IV) phenylphosphonate was synthesized by slowly adding an aqueous solution of 0.1 *M* uranium(IV) chloride to one 0.8 *M* phenylphosphonic acid maintained at 40°C and constantly stirred. The final P : U molar ratio was 10 : 1. The temperature and stirring were continued for 1/2 hr more. The resulting light-blue solid was isolated by centrifugation, washed with acetone, and air dried. The uranium(IV) chloride solution was obtained by electrolytic reduction of uranyl chloride in hydrochloric or perchloric acid medium. Uranium(IV) solution must be acid to avoid the hydrolysis leading to another species, and should be used immediately as U(IV) is easily oxidized to U(VI).

Another synthesis of uranium(IV) phenylphosphonate was carried out under the same conditions given above except for the addition of ascorbic acid (4 mg/ml at intervals of 15 min) and an increase in the temperature to 60°C. Adding ascorbic acid avoided the oxidation of U(IV) to U(VI) that occurs at higher temperatures. This synthesis led to a product that had the same chemical formula but was slightly more crystalline. We used this solid, with sharper diffraction lines, for the structural study by X-ray powder diffraction. Attempts to grow single crystals by keeping the reaction mixture for a long time or increasing temperature resulted in a uranyl(VI) phenylphosphonate or a mixed uranyl(VI) uranium(IV) phenylphosphonate.

Uranium(IV) pyrophosphate is the thermal decomposition product of uranium(IV) phenylphosphonate. UP_2O_7 was synthesized by heating $U(O_3PC_6H_5)_2$ at 800°C for one day.

X-ray powder diffraction studies (XRD) were performed on a Siemens D-501 automated diffractometer using graphite-monochromated Cu$K\alpha$ radiation. The powder pattern for the structural study of $U(O_3PC_6H_5)_2$ was recorded between 10° and 100° (2Θ), in 0.03° steps, with a counting time of 15 sec per step (the X-ray tube was operating at 40 kV and 22 mA). The powder pattern of UP_2O_7 was recorded between 14° and 96° (2Θ), in 0.03° steps, with a counting time of 15 sec per step. The data were transferred to a VAX computer for Rietveld (18) analysis by the GSAS program (19) using a pseudo-Voight peak shape function. Infrared spectra were recorded on a Perkin-Elmer 883 spectrometer with a spectral range of 4000–200 cm^{-1}, using dry KBr pellets containing 2% of the sample. The absorption spectra were recorded on a Shimadzu UV-3100 in the 400–1700 nm range, with $BaSO_4$ as reference standard. Thermal analysis (TGA and DTA) was carried out in air on a Rigaku Thermoflex apparatus at a heating rate of 10 K min^{-1} with calcined Al_2O_3 as the internal standard reference. Elemental analysis (C, H) was carried out in a Perkin-Elmer 240C analyzer.

TABLE 1
X-Ray Diffraction Data for $U(O_3PC_6H_5)_2$

d_{obs} (Å)	d_{cal} (Å)	*h k l*	$I/I_0 \times 100$
14.886	14.855	0 0 1	100
7.430	7.428	0 0 2	24
4.956	4.952	0 0 3	17
4.849	4.850	1 1 0	12
4.689	4.692, 4.691	−1 1 1, 2 0 0	53
4.335	4.335	2 0 1	28
4.173	4.185, 4.174	−2 0 2, −1 1 2	31
3.955	3.957	1 1 2	12
3.778	3.779	2 0 2	12
3.571	3.571	−1 1 3	22
3.369	3.368	1 1 3	7
3.224	3.229	2 0 3	7
3.034	3.035	−1 1 4	12
2.871	2.869	1 1 4	7
2.833	2.833	0 2 0	7
2.783	2.783	0 2 1	10
2.741	2.741, 2.738	−3 1 1, 3 1 0	18
2.650	2.649, 2.647, 2.646	−2 0 5, 0 2 2, 3 1 1	16
2.600	2.602	−1 1 5	9
2.493	2.490	3 1 2	6

The uranium content for $U(O_3PC_6H_5)_2$ was determined gravimetrically by dissolving the sample in sulfuric acid (1 : 1), precipitating the uranium with cupferron, and finally roasting it to U_3O_8. The phosphorus content was determined colorimetrically as molybdophosphate complex. The carbon and hydrogen contents were determined by elemental chemical analysis. The results were: U, 43.1%; P, 11.2%; C, 28.2%; H 2.1%. Calculated for $U(O_3PC_6H_5)_2$ the results were: U, 43.3%; P, 11.3%; C, 26.2%; H 1.8%. UP_2O_7 was identified by its powder diffraction pattern (20).

RESULTS

Structural Study of $U(O_3PC_6H_5)_2$

The X-ray powder diffraction pattern (Table 1) was auto-indexed by using the Lattparm program (21), based on the Visser algorithm (22), from the position of the first 20 reflections. The result was a monoclinic unit cell (a = 9.443 Å, b = 5.666 Å, c = 14.95 Å, β = 96.48°, V = 794.8 $Å^3$, Z = 2, and V (nonhydrogen atoms) =

18.9 Å^3/atom) with a figure of merit, M_{20}, of 33 (23). This cell accounted for all the observed peaks in the pattern. Systematic absences were consistent with a C-centered unit cell, with no further absence conditions. The centrosymmetric space group $C2/m$ was assumed for the subsequent data analysis.

The derived unit cell for $U(O_3PC_6H_5)_2$ is related to that of $Zr(O_3PC_6H_5)_2$ (a = 9.10 Å, b = 5.42 Å, c = 30.23 Å, β = 101.33°) (11), showing a close structural relationship. However, the c-axis of the Zr derivative is doubled, leading to a different space group, $C2/c$. As the cell dimensions and the space groups were different, we attempted to solve the crystal structure of $U(O_3PC_6H_5)_2$ *ab inito* by using powder diffraction data.

The pattern decomposition option (24) of the GSAS (19) package was used to extract integrated intensities from a limited region of the powder pattern ($10 < 2\Theta < 35.4°$). A total of 42 reflections were used as input to create a Patterson map by using the SHELXS program. The position of uranium at (000) was easily derived from this map. With this position, we came back to the Rietveld method. The inclusion of uranium resulted in R_{WP} = 31% (R factor defined in Refs. (18) and (19)). The position of the phosphorus atom was obtained from a difference Fourier map at the mirror plane ($x0z$) with $x \approx 0.35$ and $z \approx 0.10$. The inclusion of this atom dropped R_{WP} to 21%, and another difference of Fourier map revealed the position of the oxygen atoms. Rietveld refinement of the $U(O_3P)_2$ framework gave R_{WP} = 16.6%. At this stage, further difference Fourier maps did not reveal the phenyl ring. This was due to the presence of a very heavy atom in the structure (uranium), which masks the contribution of the light atoms (carbons) and the disorder of the phenyl rings (see below).

The first reflection (001) atom ≈15 Å had to be omitted from the refinement due to its high asymmetry. Initially, we refined the overall parameters (scale factor, unit cell parameters, zero-point error, and peak shape parameters), and the background was fitted manually. Later, atomic positions were refined with soft constraints in the P–O bonds, 1.53(2) Å. The refined O(1)–P–O(1) and O(1)–P–O(2) angles ranged between 112° and 103°. At this stage, we decided to include the phenyl group in the possible theoretical positions. As the P and O(2) atoms lie in the special position at ($x0z$), C(1) has to lie in the same mirror plane at a theoretical distance of ≈1.80 Å and with C(1)–P–O angles close to 110°. These two conditions are enough to fix the C(1) position. The angle between the direction of the P–C(1) bond and the c-axis was ≈10°.

If the phenyl groups are not disordered, the flat rings should lie in the *ac* plane or in the plane perpendicular to this that is tilted out 10° from the *bc* plane. Starting from the position of C(1), we built two models with the C6 flat hexagonal ring in these two perpendicular planes, assuming C–C bond distances of 1.40 Å and C–C–C angles of 120°. Including the phenyl group at the *ac* and ⊥-*ac* planes, R_{WP} was dropped from 16.6% to 11.8 and 10.0%, respectively. These better R-factors show that the fit was improved notably.

However, due to the high degree of rotational freedom along the P–C(1) bond, the phenyl rings may be rotated out in an intermediate position between the *ac* plane and the ⊥-*ac* plane. This would break the mirror plane symmetry at a local level, but the random disorder at long distances would result in the observed symmetry. We modeled this possibility by refining the occupation factors of the *ac* and ⊥-*ac* models, constrained to give an overall full occupancy, 100%. In fact, refining the occupation fraction of these two orthogonal components, we were refining the angle between the flat aromatic ring and the *ac* plane. This model further improved the fit, and R_{WP} fell to 8.0%. Due to the disorder of the phenyl groups, and the presence of uranium, the refinement of the position of the carbons was slightly unstable. As the geometry of the phenyl groups is well known in phosphonates (2b, 2c, 2c, 3a, 3b, 9), we decided do not refine the positions of the carbon atoms, leaving them at the theoretical ones. The final model is given in Table 2. C(1) and C(6) are situated in the interjection line of the orthogonal planes. Hence, their occupation factors are 1.0 and were not refined, as they are not disordered. The carbons in *ortho* and *meta* positions are not on the *ac* plane and they are disordered.

The final refinement converged to R_{WP} = 8.0%, R_P = 6.0%, and R_F = 3.0%. Results of refinement are given in Table 2, and the final observed, calculated, and difference profiles are given in Fig. 1. The refined bond distances and angles are showed in Table 3.

Infrared Spectroscopy Study

The IR spectra of $U(O_3PC_6H_5)_2$ and $Zr(O_3PC_6H_5)_2$ are shown in Fig. 2. The IR data of the latter compound are given for the sake of comparison. There are not bands in the O–H stretching and H–O-H bending regions at ≈3500–3200 cm^{-1} and ≈1630 cm^{-1}, respectively. The C–H stretching vibrations of the phenyl ring are present around 3000 cm^{-1}. At approximately 1400 cm^{-1}, the C–C aromatic stretching bands appear. The intense band at ≈1160 cm^{-1} is due to the P–C stretching band, and the broad band at ≈1050 cm^{-1} is due to the P–O stretching vibrations (25). At lower frequencies, bands appear due to the bending vibrations of the different groups present in these compounds.

Diffuse Reflectance Spectra

The absorption spectrum of uranium phenylphosphonate is shown in Fig. 3. Main absorption lines due to tetravalent uranium ($5f^2$) spread from about 400 nm up to 1500 nm. In octahedral symmetry the electric dipole transi-

TABLE 2
Final Unit Cell and Structural Parameters for $U(O_3PC_6H_5)_2$ in Space Group $C2/m$

Unit cell parameters

a = 9.4559(7) Å	b = 5.6769(5) Å	c = 14.9687(12) Å	β = 96.539(5) Å
V = 798.3(1) Å^3	Z = 2	V_{at} = 19.0 Å^3/at	

Structural parameters

Atom	Sym. position	x	y	z	Fraction	U_{iso} (Å^2)
U	2*a*	0.00	0.00	0.00	1.00	0.0003(9)
P	4*i*	0.3629(11)	0.00	0.1173(5)	1.00	0.008(2)
O(1)	8*j*	−0.0494(12)	0.2747(16)	0.1067(7)	1.00	0.008(−)
O(2)	4*i*	0.2162(13)	0.00	0.0617(12)	1.00	0.008(−)
C(1)	4*i*	0.325	0.00	0.230	1.00	0.028(7)
C(2)	4*i*	0.187	0.00	0.255	0.41(1)	0.028(−)
C(3)	4*i*	0.440	0.00	0.298	0.41(−)	0.028(−)
C(4)	4*i*	0.168	0.00	0.346	0.41(−)	0.028(−)
C(5)	4*i*	0.420	0.00	0.390	0.41(−)	0.028(−)
C(6)	4*i*	0.283	0.00	0.415	1.00	0.028(−)
C(2′)	8*j*	0.315	0.212	0.276	0.59(−)	0.028(−)
C(3′)	8*j*	0.295	0.212	0.368	0.59(−)	0.028(−)

tions $f \rightarrow f$ are strongly forbidden, but they are observed due to vibronic coupling. This behavior is clearly observed in the spectrum as there are four bands in the near-IR region which corresponds to $^3H_5$, $^3F_4$, and $^3F_3$ states (see Table 4). At 1675 nm an overtone C–H from phenyl groups is observed. The absorption bands in the VIS region are mainly vibronic in character, and these may be attributed to $^3H_6$, $^3P_0$, $^1G_4$, $^1D_2$, $^3P_1$, $^1I_6$, and $^3P_2$ states. The shape and relative intensities of the bands are closely similar to $CsUCl_6$ (26) and the uranium(IV) uranyl (VI) phosphate (27) described in the literature. In Fig. 3 is also shown the spectra of uranium(IV) pyrophosphate. In Table 4 the observed bands and their assignments for both compounds are given.

Thermal Analysis Study

The TGA–DTA curves for $U(O_3PC_6H_5)_2$ are shown in Fig. 4. The shape of the curve is quite simple as only one process is detected. The exothermic effect at approxi-

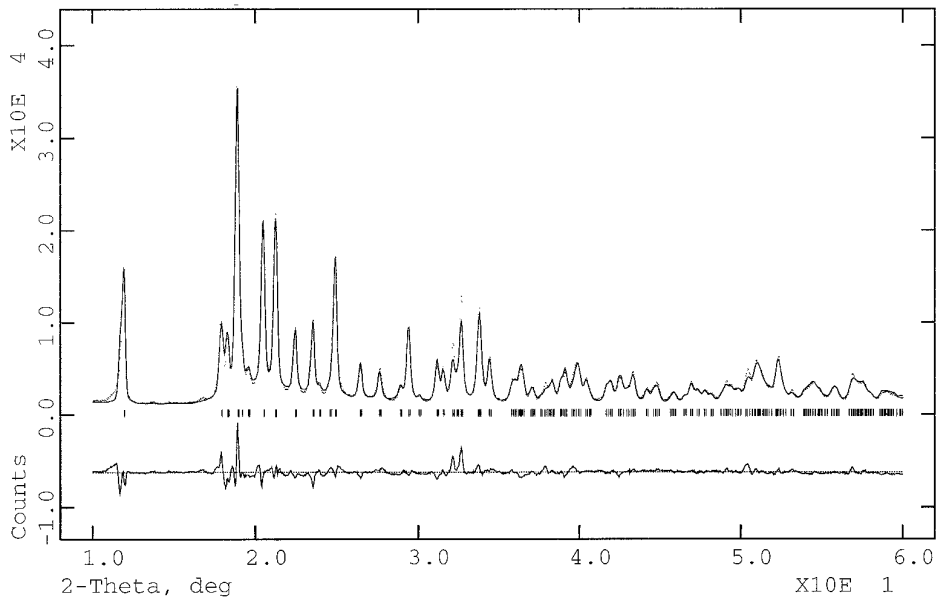

FIG. 1. Final observed (points), calculated (full line), and difference X-ray diffraction profiles for $U(O_3PC_6H_5)_2$ with the reflections allowed for the space group marked at the bottom.

TABLE 3
Bond Lengths (Å) and Angles (°) for $U(O_3PC_6H_5)_2$

U–O(1) 4*x*	2.318(9)	O(1)–U–O(1) 2*x*	95.4(6)
U–O(2) 2*x*	2.145(11)	O(1)–U–O(1) 2*x*	180.0
		O(1)–U–O(1) 2*x*	84.6(6)
		O(1)–U–O(2) 4*x*	87.7(5)
		O(1)–U–O(2) 4*x*	92.3(5)
		O(2)–U–O(2)	180.0
P–O(1) 2*x*	1.542(3)	O(1)–P–O(1)	112.1(12)
P–O(2)	1.535(5)	O(1)–P–O(2) 2*x*	114.1(6)
P–C(1)	1.764(9)	O(1)–P–C(1) 2*x*	105.6(6)
		O(2)–P–C(1)	104.4(11)
		U–O(1)–P	141.4(7)
		U–O(2)–P	172.7(15)

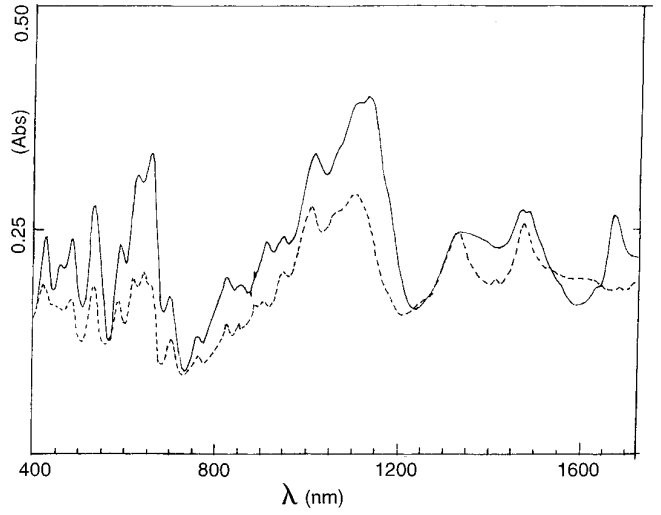

FIG. 3. Absorption spectra for (solid line) $U(O_3PC_6H_5)_2$ and (dotted line) UP_2O_7.

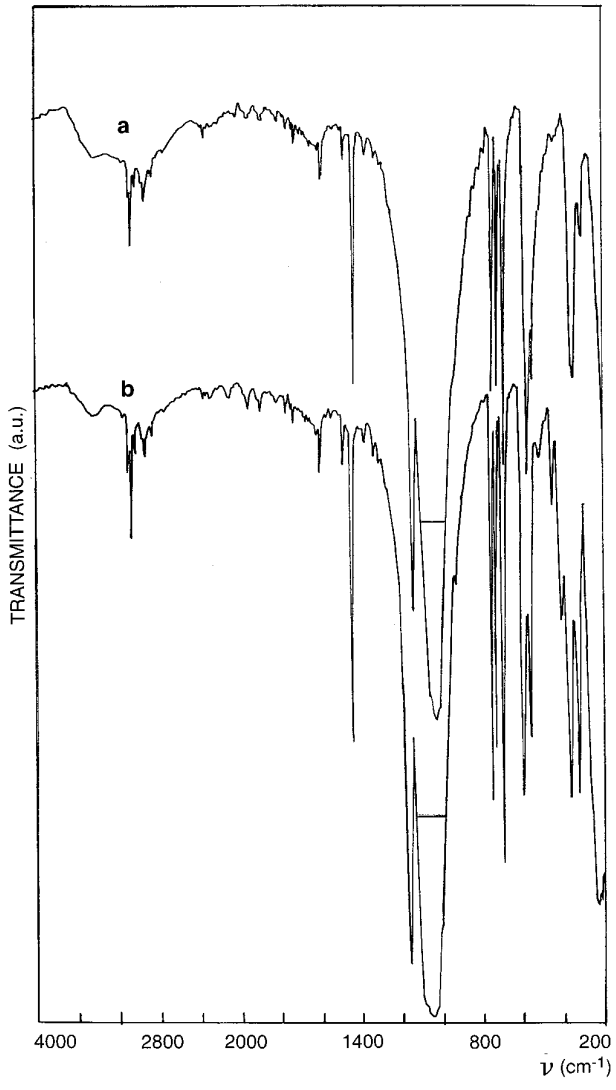

FIG. 2. IR spectra for (a) $U(O_3PC_6H_5)_2$ and (b) $Zr(O_3PC_6H_5)_2$.

mately 500°C, associated with a weight loss of 28%, is due to the combustion of the organic matter. The temperature of this exotherm shows the high thermal stability of this compound. The product obtained after the heating process was uranium(IV) pyrophosphate, UP_2O_7, identified by its powder diffraction pattern (20). The theoretical weight loss of this process is 25%. An increase of weight due to the oxidation of U(IV) to U(VI) was not detected, which confirms that the final product contains U(IV).

TABLE 4
VIS-near-IR Data $U(O_3PC_6H_5)_2$ and UP_2O_7

$U(O_3PC_6H_5)_2$		UP_2O_7	
Band (nm)	Assignment	Band (nm)	Assignment
1676	Overtone C–H	—	—
1490	$^3H_5$	1480 1334	$^3H_5$
1134 1100	$^3F_4$	1111	$^3F_4$
1020	$^3F_3$	1012 950	$^3F_3$
760	$^3H_6$	820	$^3H_6$
700	$^3P_0$	708	$^3P_0$
659 624 590	$^1G_4$ $^1D_2$ $^1G_4$	647 620 590	$^1G_4$ $^1D_2$ $^1G_4$
532	$^3P_1$	532	$^3P_1$
485 463	$^1I_6$	485 463	$^1I_6$
425 417	$^3P_2$	425 417	$^3P_2$

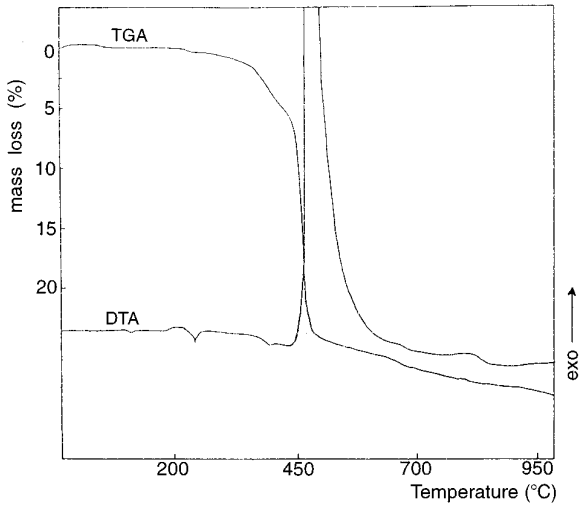

FIG. 4. TGA and DTA curves for $U(O_3PC_6H_5)_2$.

Structural Study of UP_2O_7

The X-ray powder diffraction pattern of the thermal decomposition product of $U(O_3PC_6H_5)_2$ matches that of UP_2O_7 (PDF No. 16-233). The crystal structure of UP_2O_7 was partially studied (16), and it is known that it crystallizes in the cubic ZrP_2O_7-type structure. We have used the structure of ZrP_2O_7 (17) as starting model in the $Pa\bar{3}$ for a Rietveld refinement using powder X-ray diffraction data. First, the overall parameters (scale factor, background coefficients, unit cell parameters, zero-point error, and peak shape parameters) were refined. Second, atomic parameters (positionals and isotropic temperature factors) were refined. At this stage, the isotropic temperature factor of the oxygen that bridges the pyrophosphate groups was anomalously high, U_{iso} O(1) = 0.15(1) Å^2. This oxygen is located at (1/2, 1/2, 1/2) to give a linear P–O(1)–P group. It is known that oxygens bridging pyrophosphates (28) and pyro arsenate (29) groups, that should result in linear X–O–X groups, usually present static disorder to give an angular X–O–X bond.

Hence, the large isotropic temperature factor of O(1) is due to static disorder around the ideal position (1/2, 1/2, 1/2) rather than thermal vibration. We attempted to model the disorder in a chemically realistic way by refining the position of O(1) in (x, $-x$, 1/2), which results in 6 possible positions equidistant from the phosphorus atoms, and with a multiplicity of 0.167. A free refinement of the thermal factor of this oxygen converged to $-0.02(1)$, an unrealistic negative value, although quite close to zero. In the final model we constrained the temperature factors for the two oxygens to have the same value, and this converged to R_{WP} = 11.7%, R_P = 8.6%, and R_F = 10.4%. Results of refinement are given in Table 5, and the final observed, calculated, and difference profiles are given in Fig. 5. The refined bond distances and angles are showed in Table 6.

DISCUSSION

$U(O_3PC_6H_5)_2$

The high crystallinity of this compound has allowed us to auto index its X-ray powder pattern. The quality of the pattern was also enough to attain success in the *ab initio* procedure. From a combination of Patterson and difference Fourier maps, we have determined the framework of the $U(O_3P)_2$ layers. The position and orientation of the phenyl groups have been estimated from the combination of modeling and Rietveld techniques.

The lamellar structure of uranium(IV) phenyl phosphonate is very similar to those of α-$Zr(HPO_4)_2 \cdot H_2O$ and $Zr(O_3PC_6H_5)_2$. The layers are formed of α-$M(O_3PX)_2$ groups with X equal to oxygen for the phosphate and to carbon for the phosphonates. The U atoms are located in planes at z = 0 and 1. In a given layer, three U atoms form a pseudo-equilateral triangle, and the P atoms are situated just at the center of these triangles, approximately 1.7 Å above or below the plane. This is the same layer arrangement present in α-$Zr(O_3POH)_2 \cdot H_2O$ (12) and zir-

TABLE 5
Final Unit Cell and Structural Parameters for UP_2O_7 in Space Group $Pa\bar{3}$

Unit cell parameters

a = 8.6311(2) Å	V = 642.99(4) Å^3	Z = 4	V_{at} = 16.1 Å^3/atom

Structural parameters

Atom	Sym. position	x	y	z	Fraction	U_{iso} (Å^2)
U	4a	0.00	0.00	0.00	1.00	0.0167(4)
P	8c	0.4014(6)	0.4014(6)	0.4014(6)	1.00	0.033(3)
O(1)	24d	0.548(2)	0.452(2)	0.50	0.167	0.048(4)
O(2)	24d	0.4487(11)	0.2455(8)	0.4321(13)	1.00	0.048(−)

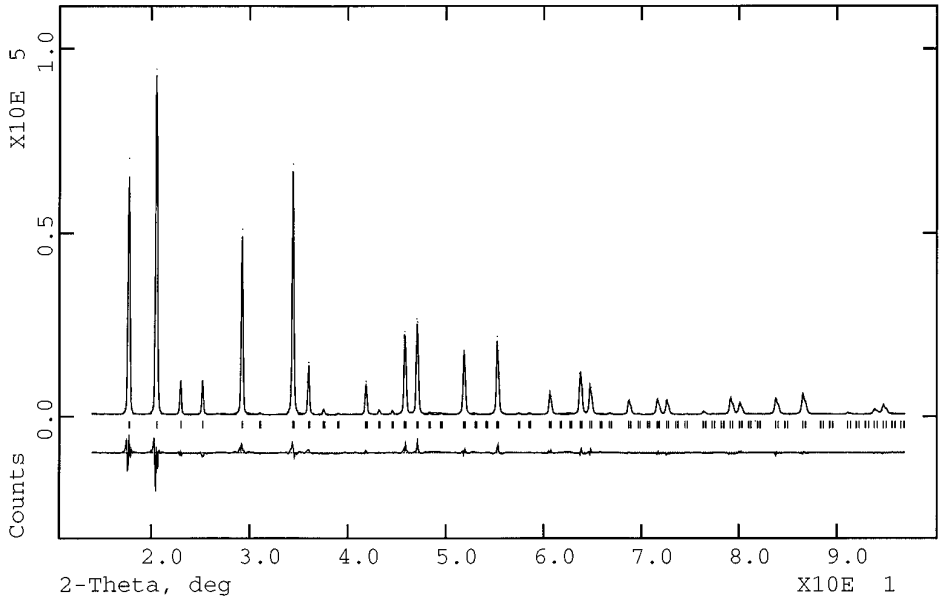

FIG. 5. Final observed (points), calculated (full line), and difference X-ray diffraction profiles for UP_2O_7, with the reflections allowed for the space group marked at the bottom.

conium phenyl phosphonate (11). The main difference in the layers of these three compounds is their crystal symmetry. α-ZrP crystallizes in the $P2_1/n$ space group (12), with Zr, P, and O atoms in general positions. $Zr(O_3PC_6H_5)_2$ crystallizes in the $C2/c$ space group, with Zr at the special position (3/4, 1/4, 1/2); and P, O, and C(1) in general positions (11). In this two structures the *c*-axis is doubled. $U(O_3PC_6H_5)_2$ crystallizes in the $C2/m$ space group, and the *c*-axis does not need to be doubled. U lies in the special position (0,0,0); P, O(2), and C(1) lie at the mirror plane at $(x,0,z)$; O(1) lies in a general position. Hence, the phosphonate groups have higher symmetry in $U(O_3PC_6H_5)_2$ (Cs symmetry) than in $Zr(O_3PC_6H_5)_2$ (C1), and this is evident in the IR spectra of both compounds (see below).

The crystal structure of $U(O_3PC_6H_5)_2$ is depicted in Fig. 6. The uranium atoms have an octahedral environment of oxygens, with U–O bond distance of 4×2.32 Å, and 2×2.15 Å. The phosphonate groups are tetrahedral with reasonable P–O bond distances and O–P–O angles close to 110°. The phenyl rings are situated in the interlamellar space and form an angle of 10° with the *c*-axis direction. In Fig. 6 the disorder of the phenyl groups is not shown, instead a view of the $\perp$-*ac* model is given. From the refined occupational fraction of the carbons in the *ac* and $\perp$-*ac* models, we can derive the angle between the flat phenyl group and the *ac* plane. The rotation angle along the P–C(1) bond was 53° out of the *ac* plane. Although at a molecular level, the phenyl groups violate the mirror plane symmetry, the random disorder of the phenyl groups at long distances would result in the observed symmetry, a mirror plane at $(x\,0\,z)$. Disorder of the phenyl rings has been reported several times in metal phosphonates (2b, 2c).

TABLE 6
Bond Lengths (Å) and Angles (°) for UP_2O_7

U–O(2) 6*x*	2.243(7)	O(2)–U–O(2) 6*x*	89.5(4)
		O(2)–U–O(2) 3*x*	180.0
		O(2)–U–O(2) 6*x*	90.5(4)
P–O(1)	1.59(1)	O(1)–P–O(2)	86(1)
P–O(2) 3*x*	1.43(1)	O(1)–P–O(2)	106(1)
		O(1)–P–O(2)	123(1)
		O(2)–P–O(2) 3*x*	113.0(5)
		P–O(1)–P	136(2)
		U–O(2)–P	173(1)

Very useful information can be extracted from the IR spectra of $U(O_3PC_6H_5)_2$ and $Zr(O_3PC_6H_5)_2$, in addition to the assignment of the different bands (Fig. 2). (i) The absence of O–H stretching and H–O–H bending vibrations corroborates that these compounds crystallize without hydration water. (ii) The absence of bands in the IR spectrum of $U(O_3PC_6H_5)_2$ between 900 and 830 cm^{-1} confirms that U(VI) is not formed in the synthesis, as the characteristic stretching bands of the uranyl(VI) groups appear in that region. (iii) Last but not least, the comparison of the width of the P–O stretching vibrations bands in $M(O_3PC_6H_5)_2$ (M = U, Zr) can give some insight into the symmetry of the phosphonate groups. From our struc-

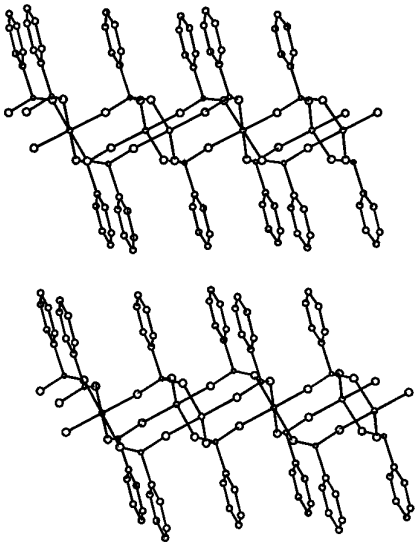

FIG. 6. [010] ORTEP view of the crystal structure of $U(O_3PC_6H_5)_2$. The disorder has been omitted for the sake of clarity. The $\perp$-*ac* model is displayed.

tural study for M = U, the phosphonate group has a mirror plane symmetry (Cs, see Table 3), and from the reported structure for M = Zr, the phosphonate group has no symmetry (C1) (11). Hence, the PO_3C groups are more regular for M = U than for M = Zr. This is evident from the IR spectra (Fig. 2), as the width of the P–O stretching bands

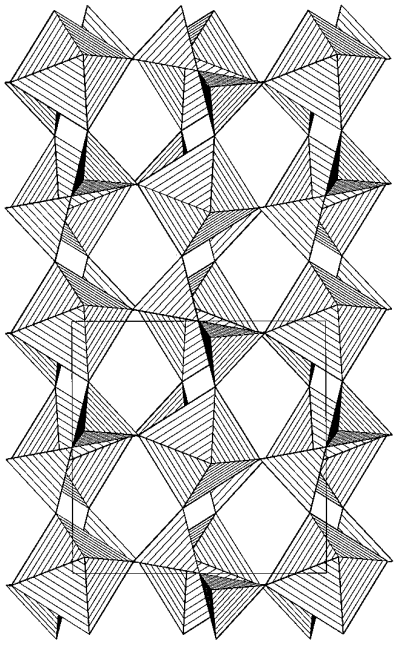

FIG. 7. STRUPLO view of the framework of UP_2O_7. The disorder of the oxygens that bridge the pyro groups is not shown.

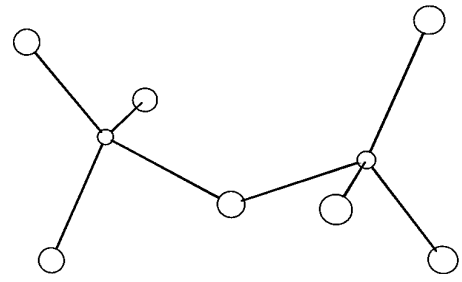

FIG. 8. ORTEP view of one pyro group shown the angular *X–O–X* bridge.

(at 2/3 of the transmittance of the band for both compounds) is 118 cm^{-1} for M = U and 142 cm^{-1} for M = Zr.

UP_2O_7

This compound belongs to the cubic ZrP_2O_7-type structure. The crystal structure is shown in Fig. 7. The uranium atoms have an octahedral environment of oxygens. The U(IV) octahedra are linked together through six different pyrophosphate groups to give the three-dimensional network. The main feature of this compound is the static disorder of the oxygen that bridges the pyro phosphate groups.

We have modeled the disorder of these oxygens by refining out of the ideal position, constrained to be equidistant to the two phosphorus atoms (Fig. 8). With this condition, the isotropic temperature factor drops to a negative value although quite close to zero. This may be a consequence of improper modeling of the disorder, and a short-range order of the oxygen disorder may occur. A synchrotron single-crystal study (30) of cubic MoP_2O_7 revealed superlattice reflections, and the cell parameters had to be tripled to index those peaks. With the medium resolution data we have, superlattice reflections have not been observed, and we cannot study the possible ordering of these oxygens. Hence, the model for the disorder we propose is only approximate and may be the responsible of some angles of the pyrophosphate groups (86° and 123°) that are too far off the tetrahedral angle $\approx$110°.

The absorption spectra of both compounds $U(O_3PC_6H_5)_2$ and UP_2O_7 are quite similar (see Fig. 3 and Table 4). The data are fully compatible with U(IV) in a pseudo-octahedral oxygen coordination. The uranium environment in the pyrophosphate is more symmetrical and hence, the bands have slightly lower intensity.

ACKNOWLEDGMENTS

We thank DGICYT (Ministerio de Educación y Ciencia) for financial support through research project PB-93/1245.

REFERENCES

1. (a) C. M. Mikulski, N. M. Karayannis, J. V. Minkiewicz, L. L. Pytlewski, and M. M. Labes, *Inorg. Chim. Acta* **3,** 523 (1996); (b) S. Yamanaka, *Inorg. Chem.* **15,** 2811 (1976); (c) G. Alberti, U. Costantino, S. Allulli, and J. Tommassini, *J. Inorg. Nucl. Chem.* **40,** 1113 (1978); (d) M. B. Dines, R. E. Cooksey, P. C. Griffith, and R. H. Lane, *Inorg. Chem.* **22,** 1003 (1983); (e) Y. Ortiz-Avila and A. Clearfield, *J. Chem. Soc. Dalton Trans.,* 1617 (1989); (f) G. Alberti, U. Costantino, F. Marmottini, R. Vivani, and P. Zappelli, *Angew. Chem. Int. Ed. Engl.* **32,** 1357 (1993).
2. (a) D. Cunningham, P. J. D. Hennelly, and T. Deeney, *Inorg. Chim. Acta* **37,** 95 (1979); (b) G. Cao, H. Lee, V. M. Lynch, and T. E. Mallouk, *Inorg. Chem.* **27,** 2781 (1988); (c) K. Martin, P. J. Squattrito, and A. Clearfield, *Inorg. Chim. Acta* **155,** 7 (1989); (d) G. Cao, V. M. Lynch, J. S. Swinnea, and T. E. Mallouk, *Inorg. Chem.* **29,** 2112 (1990); (e) Y. Zhang and A. Clearfield, *Inorg. Chem.* **31,** 2821 (1992); (f) J. Bideau, C. Payen, P. Palvadeau, and B. Bujoli, *Inorg. Chem.* **33,** 4885 (1994).
3. (a) B. Bujoli, P. Palvadeau, and J. Rouxel, *Chem. Mater.* **2,** 582 (1990). (b) R. Wang, Y. Zhang, H. Hu, R. R. Frausto, and A. Clearfield, *Chem. Mater.* **4,** 864 (1992).
4. L. Moreno and F. M. Cantero, ''Niobium(V) Phenyl Phosphonate,'' unpublished.
5. M. E. Thompson, *Chem. Mater.* **6,** 1168 (1994).
6. (a) J. W. Johnson, J. F. Brody, R. M. Alexander, B. Pilarski, and A. L. Katritzky, *Chem. Mater.* **2,** 198 (1990); (b) G. Cao and T. E. Mallouk, *Inorg. Chem.* **30,** 1434 (1991); (c) K. J. Frink, R. Wang, J. L. Colon, and A. Clearfield, *Inorg. Chem.* **30,** 1438 (1991).
7. (a) S. Cheng, G. Z. Peng, and A. Clearfield, *Ind. Eng. Chem. Prod. Res. Dev.* **23,** 219 (1984); (b) G. Z. Peng and A. Clearfield, *J. Inclusion Phenom.* **6,** 49 (1988).
8. (a) M. Casciola, U. Costantino, S. Fazzini, and G. Tosoratti, *Solid State Ionics* **8,** 27 (1983); (b) G. Alberti, M. Casciola, R. Palombari, and A. Peraio, *Solid State Ionics* **58,** 339 (1992).
9. J. L. Colon, C. Y. Yang, A. Clearfield, and C. R. Martin, *J. Phys. Chem.* **92,** 5777 (1988).
10. (a) P. R. Rudolf, C. Saldarriaga-Molina, and A. Clearfield, *J. Phys. Chem.* **90,** 6122 (1986); (b) A. K. Cheetham and A. P. Wilkinson, *J. Phys. Chem. Solids* **52,** 1199 (1991); (c) A. K. Cheetham and A. P. Wilkinson, *Angew. Chem. Int. Ed. Engl.* **31,** 1557 (1992).
11. M. D. Poojary, H. L. Hu, F. L. Campbell III, and A. Clearfield, *Acta Crystallogr.* **B49,** 996 (1993).
12. (a) A. Clearfield and G. D. Smith, *Inorg. Chem.* **8,** 431 (1969); (b) J. M. Troup and A. Clearfield, *Inorg. Chem.* **16,** 3311 (1977).
13. G. Huan, A. J. Jacobson, J. W. Johnson, and E. W. Corcoran, *Chem. Mater.* **2,** 91 (1990).
14. R. Gopal and C. Calvo, *J. Solid State Chem.* **5,** 432 (1972).
15. A. Cabeza and S. Bruque, unpublished.
16. G. Peyronel, *Z. Kristallogr.* **94,** 311 (1936).
17. C. Huang, O. Knop, D. A. Othen, F. W. D. Woodhams, and R. A. Howei, *Can. J. Chem.* **53,** 79 (1975).
18. (a) H. M. Rietveld, *J. Appl. Crystallogr.* **2,** 65 (1969); (b) ''The Rietveld Method'' (R. A. Young, Ed.). Oxford Univ. Press, Oxford, 1993.
19. A. C. Larson, and R. B. Von Dreele, Los Alamos National Laboratory, Report LA-UR-86-748, 1987.
20. B. Burdese, *Ann. Chim.* (*Rome*) **53,** 333 (1963).
21. R. Garvey, ''LATTPARM Autoindexing Program.'' Department of Chemistry, North Dakota State University, Fargo, ND 58105-5516; see also R. Garvey, *Powder Diff.* **1,** 114 (1986).
22. J. W. Visser, *J. Appl. Crystallogr.* **2,** 89 (1969).
23. P. M. de Wolff, *J. Appl. Crystallogr.* **1,** 108 (1968).
24. A. LeBail, H. Duroy, and L. Fourquet, *Mater. Res. Bull.* **23,** 447 (1988).
25. Nakamoto, K. ''Infrared Spectra of Inorganic and Coordination Compounds,'' 4th ed. Wiley–Interscience, New York, 1986.
26. ''Gmelin Handbook of Inorganic Chemistry,'' Supp. Volume A5, Uranium, p. 84, 1982.
27. P. Bérnard, D. Louër, N. Dacheux, V. Brandel, and M. Genet. *Chem. Mater.* **6,** 1049–1058 (1994).
28. T. Stefanids and A. G. Nord, *Acta Crystallogr.* **C40,** 1995 (1984).
29. M. A. G. Aranda, S. Bruque, and J. P. Attfield, *Inorg. Chem.* **30,** 2043 (1991).
30. R. C. Haushalter and L. A. Mundi, *Chem. Mater.* **4,** 31 (1992).